$NaND_4C_4H_2D_2O_6.4D_2O$, the spontaneous polarization calculated only from the distortion of $ND_4^+$ cations, determined by NMR, yielded 52% of the experimental value quoted above (El Saffar & Peterson, 1976).

We are grateful to Professor A. Simon's group, MPI für Festkörperforschung, Stuttgart, for making the Guinier photographs and to Professor H. Burzlaff, Erlangen-Nürnberg University, for inspiration and helpful discussion.

### References


Aizu, K. (1971). *J. Phys. Soc. Jpn*, **31**, 1521–1526.
Aizu, K. (1984). *J. Phys. Soc. Jpn*, **53**, 1775–1782.
Aizu, K. (1986*a*). *J. Phys. Soc. Jpn*, **55**, 1663–1670.
Aizu, K. (1986*b*). *J. Phys. Soc. Jpn*, **55**, 4302–4308.
Aizu, K. (1990). *J. Phys. Soc. Jpn*, **59**, 1293–1298.
Beevers, C. A. & Hughes, W. (1941). *Proc. R. Soc. London Ser. A*, **177**, 251–259.
Brożek, Z. & Stadnicka, K. (1994). *Acta Cryst.* B**50**, 59–68.
El Saffar, Z. M. & Peterson, E. M. (1976). *J. Chem. Phys.* **64**, 3283–3290.
Iizumi, M. & Gesi, K. (1978). *J. Phys. Soc. Jpn*, **45**, 711–712.
Ishibashi, Y. & Takagi, Y. (1975). *J. Phys. Soc. Jpn*, **38**, 1715–1719.
Johnson, C. K. (1971). *ORTEP*II. Report ORNL-3794, revised. Oak Ridge National Laboratory, Tennessee, USA.
Jona, F. & Shirane, G. (1962). *Ferroelectric Crystals*. Oxford: Pergamon Press.
Kuroda, R. & Mason, F. (1981). *J. Chem. Soc. Dalton Trans.* pp. 1268–1273.
Lines, M. E. & Glass, A. M. (1977). *Principle and Applications of Ferroelectrics and Related Materials*. Oxford: Clarendon Press.
Lowry, T. M. (1964). *Optical Rotatory Power*. New York: Dover Publications.
Mucha, D. & Łasocha, W. (1994). *J. Appl. Cryst.* **27**, 201–202.
Nardelli, M. (1983). *Comput. Chem.* **7**, 95–98.
Sannikov, D. Z. & Levanyuk, A. P. (1977). *Solid State Phys.* **19**, 118–120.
Sawada, A. & Takagi, Y. (1971). *J. Phys. Soc. Jpn*, **31**, 952.
Sawada, A. & Takagi, Y. (1972). *J. Phys. Soc. Jpn*, **33**, 1071–1075.
Shkuratova, I. G., Kiosse, G. A. & Malinovskii, T. I. (1979). *Izv. Akad. Nauk SSSR, Ser. Fiz.* **43**, 1685–1690.
Takagi, Y. & Makita, Y. (1958). *J. Phys. Soc. Jpn*, **13**, 272–277.


*Acta Cryst.* (1994). B**50**, 472–479

# Structure of the Stable Phase of Methylhydrazine – First Observations of Phase Transitions

By M. Foulon, N. Lebrun, M. Muller and A. Amazzal

*Laboratoire de Dynamique et Structure des Matériaux URA CNRS* 801, *UFR de Physique, Université des Sciences et Technologies de Lille*, 59655 *Villeneuve d'Ascq CEDEX, France*

and M. T. Cohen-Adad

*Laboratoire de Physicochimie des Matériaux Luminescents, UA CNRS* 442, *Université Claude Bernard Lyon* I, 43 *boulevard du* 11 *Novembre* 1918, 69622 *Villeurbanne CEDEX, France*

(*Received* 16 *July* 1993; *accepted* 21 *March* 1994)


## Abstract

A study of methylhydrazine, $CH_3NHNH_2$, has provided the following data: monoclinic system, $P2_1/c$, $a = 10.043$ (10), $b = 3.925$ (5), $c = 7.670$ (8) Å, $\beta = 107.28$ (10)°, $V = 288.7$ (1.1) Å$^3$, $Z = 4$, $M_r = 46.07$, $D_x = 1.06$ g cm$^{-3}$, $\lambda$(Mo $K\alpha$) = 0.7107 Å, $\mu = 0.81$ cm$^{-1}$, $F(000) = 104$, $T = 179$ K, $R = 0.039$ for 703 reflexions [$I \geq 3\sigma(I)$]. A single crystal was grown *in situ* from the liquid by an adapted Bridgman method. The crystallographic cell contains equimolar proportions of isomers with the outer conformation. The internal rotation angle for the $NH_2$ group around the N—C bond is 82°. The molecular volume is estimated to be 48.9 Å$^3$, which leads to a relatively high compactness factor (0.68). The N—C molecular bonds are parallel to the crystallographic *a* axis. The structure may be described by planes of molecules, linked by van der Waals contacts, parallel to the **b**, **c** plane and related by **a**/2 translations. In each plane, one molecule is linked to four neighbours by weak hydrogen bonds. Phase transformations, as observed by DSC (differential scanning calorimetry) and Raman spectroscopy, are detailed. One glassy phase is obtained by quenching the liquid. One metastable phase appears by rapid cooling. This metastable

phase may be simulated from the stable phase as a pseudo-quadratic disordered structure. This allows an analysis of the phase transition.

## 1. Introduction

This work is part of a comprehensive interdisciplinary study on physical and chemical properties of binary mixtures of water with alkylhydrazines: hydrazine ($N_2H_4$), methylhydrazine ($CH_3NHNH_2$) and 1,1-dimethylhydrazine [$(CH_3)_2NNH_2$].

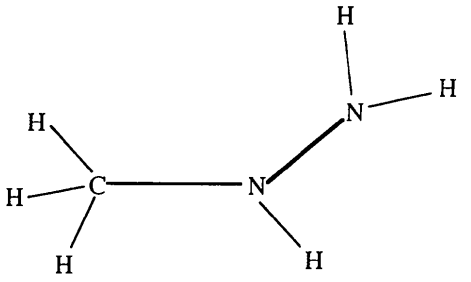


Industrial applications of alkylhydrazines are well known, as some of them are used as fuel for satellite and rocket propulsion (Wrobel & Grelecki, 1967).

Some thermodynamical and physical properties of these solutions have been explained by the existence of strong molecular interactions in the liquid phase modelled by chemical associations (Cohen-Adad, El Allali & Getzen, 1987; Ferriol *et al.*, 1993; Ferriol *et al.*, 1992; Laachach, 1989; Laachach *et al.*, 1992).

On the other hand, the existence of glassy, metastable and stable phases for alkylhydrazines and their hydrates makes these compounds of additional interest for fundamental research on condensed matter. For a given compound, the various phase transformations depend greatly on the thermal treatment, especially on the cooling and reheating rate or on the annealing time and temperature. For example, previous studies showed that the hydrazine monohydrate may be quenched easily into a glassy phase from the liquid or into a 'glassy crystal' phase from a metastable cubic phase (Foulon, Guinet, Muller, Lebrun & Fontaine, 1991; Foulon, Muller, Damien & Guinet, 1990; Foulon, Muller, Guinet, Lahlaouti, Oonk & Mittenburg, 1990). Phase transformation kinetics for methylhydrazine hydrates are much slower and permit easier experimental investigations. In the present work, DSC, Raman spectroscopy and X-ray diffraction studies on pure methylhydrazine proved that it might be quenched into a glassy liquid and can exhibit a metastable phase on cooling. Neither of these transformations had been observed previously. To take the investigation one step further, the crystalline structure of the stable phase was determined.

## 2. Experimental

### 2.1. *Origin and synthesis of methylhydrazine*

Two different samples of methylhydrazine were used. The first was synthesized by the 'Physico-Chimie Minérale II' laboratory (Lyon I) following a Raschig process (Guidice, 1989; purity 99.5%). The second was the commercial product from Aldrich Chemical Company (purity 98%).

The purity was verified by gas chromatography and mass spectrometry.

### 2.2. *Differential scanning calorimetry*

The phase transitions were characterized on a Perkin–Elmer DSC7 apparatus. Liquid methylhydrazine (8.76 mg) was introduced into an aluminium container. Measurements were performed between room temperature and 120 K with different scanning rates on cooling and reheating ($0.5\ \text{K min}^{-1} \leq dT/dt \leq 100\ \text{K min}^{-1}$).

### 2.3. *Crystal growth and X-ray analysis*

For single crystal analysis, the sample was prepared under nitrogen to avoid oxidation. Liquid methylhydrazine (*ca* 0.10 mg) was introduced by capillarity into a Lindemann tube ($\varphi = 0.5$ mm, height of liquid = *ca* 0.8 mm). The capillary was sharpened in order to favour the growth of the crystal.

Thermal treatments were performed using a Leybold–Heraeus low-temperature nitrogen gas flow device. The isothermal stability of the gaseous flux was better than 1 K and the temperature gradient between the sample and the measuring thermocouple was estimated to be $\pm 2$ K.

A single crystal was grown *in situ* on the four-circle Philips PW1100 diffractometer using an adapted Bridgman method.

Despite numerous attempts with the very pure methylhydrazine, no sufficiently high quality single crystals were obtained. On the other hand, we succeeded with the commercial product where impurities probably accelerate the kinetics of crystallization.

The single crystal growth requires three important stages:

(1) Crystallization of the liquid as a polycrystalline material in the stable phase: the crystallization rate depends on the thermal treatment. In the present case, the crystallization was accelerated by quenching the liquid below the glassy temperature (140 K) and then by repeated reheating and cooling cycles around $T = 190$ K.

(2) Obtention of a small germ: the polycrystalline material was partially melted by horizontal displacement of the capillary in a temperature gradient assured by the outer de-icing warm stream (285 K)

and the inner cold one of the low-temperature device. The difficulty was to keep a very small germ in the sharpened extremity of the capillary.

(3) Growth of the single crystal from the germ by very slow displacement of the capillary towards the low-temperature stream: several unsuccessful attempts at different temperatures allowed the estimation of the best growing temperature. The growth of a good single crystal (estimated volume: 0.10 $mm^3$), observed visually through a binocular microscope, was obtained at $T = 179$ K.

The incident X-ray beam was monochromatized [$\lambda$(Mo $K\alpha$) = 0.7107 Å] with a pirolitic graphite crystal. The lattice constants were calculated from the setting angles of 25 accurately centred reflections ($8 \le 2\theta \le 18°$). Intensities were measured by the $\omega$–$2\theta$ scanning mode. Left and right backgrounds were measured during half the scan time. Standard deviations on intensities were deduced from counting statistics. The data collection was performed in two parts ($2 < \theta \le 23$ and $23 < \theta < 34°$). In the first part, 1123 intensities were measured, leading to 442 independent reflections after averaging ($R_{int} = 0.02$). In the second range, 878 independent reflections were collected. Three reflections were always measured every 30 min. During the first part of the data collection, these reference intensities increased linearly (3.7, 4.4 and 5.1%, respectively). An average correction was applied to the intensities. All the data were corrected for Lorentz–polarization factors. Absorption ($\mu = 0.81$ $cm^{-1}$) and extinction corrections were ignored. Scattering factors of neutral atoms are approximated by exponential series from *International Tables for X-ray Crystallography* (1974, Vol. IV) and for H atoms from Stewart, Davidson & Simpson (1965).

The structure was solved by direct methods (*MULTAN*; Germain, Main & Woolfson, 1971) and refined using full-matrix least squares (*SHELX*76; Sheldrick, 1976). The six H atoms were located on a difference Fourier map (electronic density peak 0.5 e $Å^{-3}$). The refinements of positional and thermal parameters (Table 1; anisotropic for heavy atoms, isotropic for H atoms) led to $R = 3.9\%$. Details on data collection and structure refinement are reported in Table 2.*

The lattice parameters were measured during reheating from 160 to 205 K, where anomalous damage to the crystal was observed. In this temperature range, the thermal dilatation factors were estimated from the linear evolution of the lattice constants: $\alpha(a) = 77 \times 10^{-6}$, $\alpha(b) = 121 \times 10^{-6}$ and $\alpha(c) = 78 \times 10^{-6}$ $K^{-1}$ leading to $\alpha(V) = 276 \times 10^{-6}$ $K^{-1}$.

* Lists of structure factors and anisotropic displacement parameters have been deposited with the IUCr (Reference: PA0291). Copies may be obtained through The Managing Editor, International Union of Crystallography, 5 Abbey Square, Chester CH1 2HU, England.

Table 1. *Fractional atomic coordinates* ($\times 10^4$) *and temperature factors* ($Å^2 \times 10^3$) *with e.s.d.'s of heavy and* H *atoms*

$$T = \exp[-2\pi^2(h^2a^{*2}U_{11} + k^2b^{*2}U_{22} + l^2c^{*2}U_{33} + 2klb^*c^*U_{23} + 2hla^*c^*U_{13} + 2hka^*b^*U_{12})].$$

$$U_{eq} = 1/3\sum_i\sum_j U_{ij}a_i^*a_j^*\mathbf{a}_i.\mathbf{a}_j.\dagger$$

| | $x$ | $y$ | $z$ | $U_{eq}$, $U_{iso}$‡ |
|---|---|---|---|---|
| N(1) | 1902 (1) | 5498 (3) | 372 (1) | 289 (7) |
| N(2) | 1150 (1) | 7810 (2) | −1038 (1) | 286 (12) |
| C | 3352 (1) | 5470 (4) | 412 (2) | 398 (12) |
| H(N1) | 1879 (16) | 6262 (41) | 1448 (22) | 413 (37)‡ |
| H(N2)1 | 1281 (17) | 9859 (41) | −578 (21) | 392 (39)‡ |
| H(N2)2 | 262 (18) | 7284 (40) | −1259 (21) | 448 (39)‡ |
| H(C)1 | 3431 (17) | 4415 (42) | −732 (12) | 464 (41)‡ |
| H(C)2 | 3760 (17) | 7737 (45) | 521 (22) | 518 (44)‡ |
| H(C)3 | 3889 (20) | 4094 (55) | 1422 (26) | 654 (52)‡ |

† Fischer & Tillmanns (1988).

Table 2. *Data collection and refinement at* 179 K

| | |
|---|---|
| Scan width (°) | 1.33 |
| Scan speed (° $s^{-1}$) | 0.013 |
| First data collection ($2 < \theta \le 23°$) | |
| $h$ range | −12→12 |
| $k$ range | −5→5 |
| $l$ range | −9→9 |
| Second data collection ($23 < \theta < 34°$) | |
| $h$ range | −16→16 |
| $k$ range | 0→7 |
| $l$ range | 0→13 |
| No. of measured reflections | 2001 |
| No. of unique reflections | 1320 |
| No. of observed reflections [$I > 3\sigma(I)$] | 703 |
| $R$ | 0.039 |
| $wR$ | 0.041 |
| No. of variables | 52 |
| Weighting scheme | $k = 0.9244$; $E = 8 \times 10^{-4}$ |
| $\Delta\rho_{min}$ (e $Å^{-3}$) | −0.16 |
| $\Delta\rho_{max}$ (e $Å^{-3}$) | 0.18 |

## 2.4. *Raman spectroscopy*

Raman spectroscopy was performed using a triple monochromator (Coderg T800) with an experimental resolution of 1 $cm^{-1}$. The liquid methylhydrazine was introduced into a sphere (volume *ca* 500 $mm^3$). The sample was excited with the 4880 Å radiation of an $Ar^+$ laser.

The low-temperature device used was the Leybold–Heraeus apparatus described previously.

Due to heat exchange with the incident laser beam, the sample temperature is always greater (about 15 K) than that measured.

## 3. Results and discussion

### 3.1. *Phase transitions in methylhydrazine*

3.1.1. *Differential scanning calorimetry (DSC) studies.* DSC experiments prove that methylhydra-

zine exhibits different phases depending on the thermal treatment:

(*a*) Above $T = 220$ K, the compound is liquid.

(*b*) During cooling, three different phases may be observed:

(1) A stable crystalline phase after a slow cooling from the liquid ($dT/dt < 2$ K min$^{-1}$) [Fig. 1(*a*)], which melts at 220 K on reheating.

(2) A metastable solid phase obtained only by rapid cooling of the liquid ($2 < dT/dt \leq 80$ K min$^{-1}$). Depending on the cooling rate, this metastable phase transforms completely or partially in the stable solid phase [Fig. 1(*b*)].

(3) A glassy liquid phase obtained after quenching ($dT/dt > 80$ K min$^{-1}$) prohibits almost completely the former crystallizations.

(*c*) On reheating ($0.5 < dT/dt < 100$ K min$^{-1}$), after quenching, the following phase transitions [Fig. 1(*c*)] are observed:

(1) One glassy phase transition at *ca* $T = 140$ K characterized by an increase of $C_p$ ($\Delta C_p = 1.2$ J g$^{-1}$ K$^{-1}$).

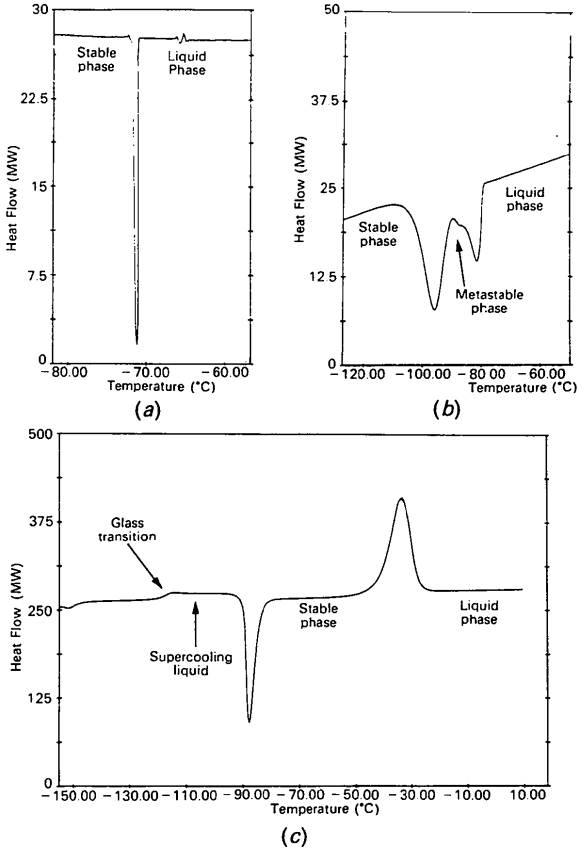


Fig. 1. DSC thermograms: (*a*) slow cooling ($dT/dt = 0.5$ K min$^{-1}$); (*b*) rapid cooling ($dT/dt = 10$ K min$^{-1}$); (*c*) reheating at $dT/dt = 40$ K min$^{-1}$ after a quenching at 40 K min$^{-1}$.

(2) The crystallization in the stable phase from a metastable liquid. This transformation depends on the heating rate ($155 < T_{tr} < 177$ K).

(3) Melting of the stable phase ($T = 220$ K with $\Delta H = 226.1$ J g$^{-1}$). This first-order transformation also exhibits an increase in specific heat ($\Delta C_p = 1.2$ J g$^{-1}$ K$^{-1}$).

### 3.1.2. *Raman spectroscopy.*

(a) First of all, Raman spectra were recorded in the low-frequency range ($15 < \nu < 350$ cm$^{-1}$) for the stable and glassy phases.

(1) In the *stable phase*, the spectra [Fig. 2(*a*)] show sharp bands corresponding to the 12 lattice modes predicted by group theory ($P2_1/c$, $Z = 4$). These active external modes may be decomposed into six translational (3 Ag + 3 Bg) and six librational modes (3 Ag + 3 Bg). However, the assignment of these low-frequency modes is difficult because of their mixed character (translational–librational coupling). Analysis *via* polarized light did not distinguish between the different symmetry modes because of the sample polycrystallinity.

(2) The *glassy phase* was obtained by quenching the liquid phase from 295 to 110 K. In this glassy phase, the large vibrational band looks like an envelope of the stable phase sharp lines and characterizes a great disorder [Fig. 2(*b*)].

(*b*) The N—H and C—H intramolecular vibrational modes were observed in the frequency range 2700–3500 cm$^{-1}$. Similar spectra were obtained for the liquid and glassy phases [Fig. 2(*c*)].

## 3.2. *Structure of the stable phase*

### 3.2.1. *Molecular geometry.*

3.2.1.1. *Previous results in the gaseous state.* Methylhydrazine may theoretically exist as three distinct rotamers (Janz & Russell, 1949): two skew forms (inner and outer) and a staggered *trans* form depending on the position of the methyl group, defined by $\theta$ on Newman projections (Fig. 3).

Previous studies show that the calculated dipole moment of the *trans* conformation ($\mu_T \cong 0.30$ Debye units) is 'very small due to cancellation of the oppositely directed lone-pair moments' (Lattimer & Harmony, 1970). Compared with the observed dipole moment of the molecule [$\mu \cong 1.70$ Debye units (Ulich, Peisker & Audrieth, 1935)], the *trans* form is improbable.

An N—N internal rotation ($\pm 180°$) exchanges the inner and outer conformers (forms 1–3 and 4–6 in Fig. 3). This rotation must avoid the *cis* conformation ($\theta = 0°$), which was found to be unstable because of the very high *cis* barrier energy value due

to the lone pair–lone pair repulsion of the two N atoms (Lattimer & Harmony, 1970).

Isomeric forms (mirror image) of the three rotamers are interchangeable, combining a torsion around the N—N bond axis (*ca* 60° rotation) and an inversion of an H atom adjacent to the methyl group.

Earlier studies led to $\theta \cong \pm 90°$ for the most probable forms (inner or outer).

The molecular conformations in the liquid and gaseous state have also been extensively studied by far-IR, microwave and Raman investigations, dipole moment (dielectric constant) measurements, determination of thermodynamic properties (calorimetry) and *ab initio* calculations (Murase, Yamamouchi, Egawa & Kuchitsu, 1991; Murase *et al.*, 1988; Yamamouchi *et al.*, 1987; Lattimer & Harmony, 1970; Aston, Fink, Janz & Russell, 1951).

The most recent studies propose the inner conformer to be more stable. A mixture of the two conformers with a small abundance of outer rotamers ($\cong$20%) was also assumed (Lattimer & Harmony, 1970).

The energy barrier for the outer conformation was estimated to be slightly higher than that for the inner one [$\Delta E \cong 300$ cm$^{-1}$ or 0.84 kcal mol$^{-1}$ (Lattimer & Harmony, 1972)].

3.2.1.2. *Molecular geometry in the stable solid phase.* The first direct Fourier transform clearly shows three peaks corresponding to the heavy atoms. The bond lengths between the central N(1) atom and the other two atoms are almost equal. This ambiguity for the relative positions of the N(2) and C atoms was easily raised by refinement.

A small residual electronic density ($\Delta\rho_{max}$ = 0.18 e Å$^{-3}$) in the same direction as the lone pairs of the two N atoms is observed.

Final bond lengths and angles are reported in Table 3. The substitution of an H atom by a methyl group in hydrazine leading to the methylhydrazine does not change the N—N bond length (Collin & Lipscomb, 1951; Foulon, 1994).

A Newman molecular projection along the N(1)—N(2) bond in the solid stable phase is drawn in Fig. 4. The molecular conformation is outer with an internal torsional angle $\theta$ of 82° (1.1). Because of the

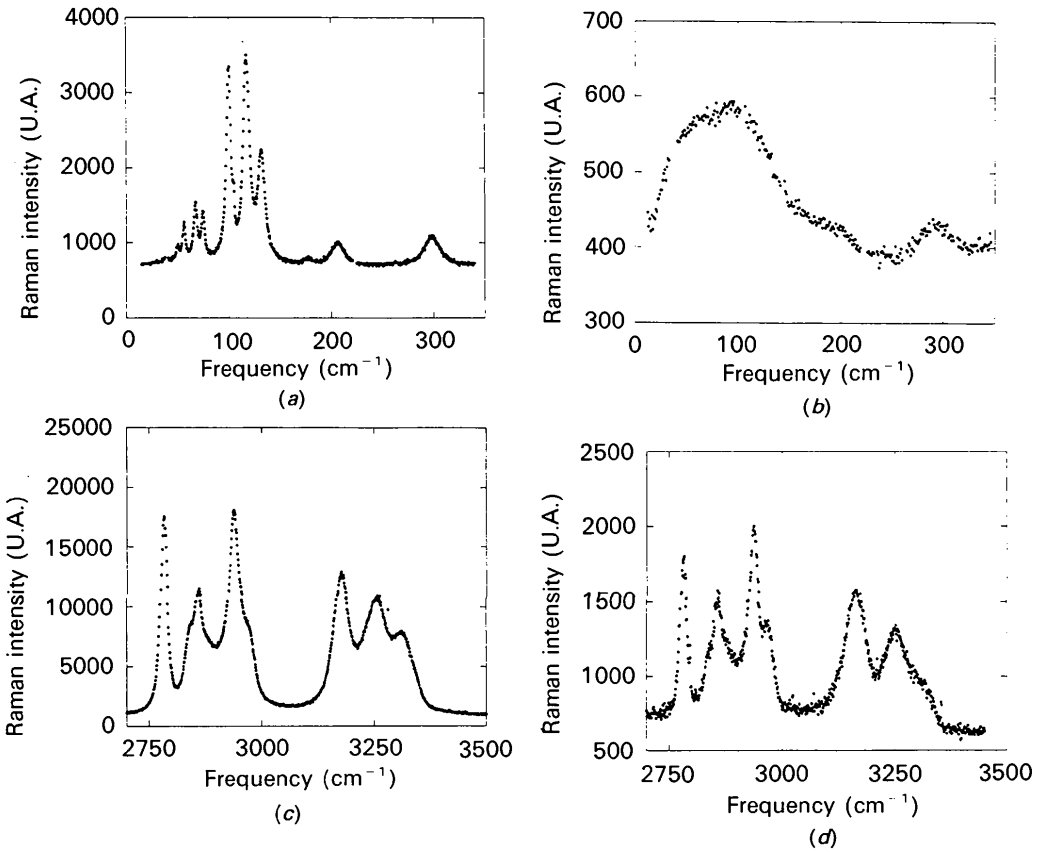


Fig. 2. Raman spectra of methylhydrazine: (*a*) stable phase at $T$ = 179 K in the range $15 < \nu < 350$ cm$^{-1}$; (*b*) glassy phase at $T$ = 110 K in the range $15 < \nu < 350$ cm$^{-1}$; (*c*) liquid ($T$ = 260 K) and (*d*) glassy phases ($T$ = 110 K) in the range $2700 < \nu < 3500$ cm$^{-1}$.

Table 3. *Bond lengths* (Å) *and angles* (°) *in the stable phase* ($T$ = 179 K) *(from last refinement)*

| | | | |
|---|---|---|---|
| N(1)—N(2) | 1.442 (2) | N(2)—N(1)—C | 108.7 (10) |
| N(1)—C | 1.447 (2) | C—N(1)—HN(1) | 106.8 (10) |
| N(1)—H(N1) | 0.885 (16) | H(N1)—N(1)—N(2) | 109.5 (10) |
| N(2)—H(N2)1 | 0.873 (16) | N(1)—N(2)—H(N2)1 | 107.1 (11) |
| N(2)—H(N2)2 | 0.881 (17) | N(1)—N(2)—H(N2)2 | 105.7 (10) |
| C—H(C)1 | 0.995 (12) | H(N2)—N(2)—H(N2)2 | 108.4 (14) |
| C—H(C)2 | 0.972 (18) | N(1)—C—H(C)1 | 109.2 (10) |
| C—H(C)3 | 0.966 (19) | N(1)—C—H(C)2 | 113.0 (9) |
| | | N(1)—C—H(C)3 | 109.9 (11) |
| | | H(C)1—C—H(C)2 | 107.6 (15) |
| | | H(C)1—C—H(C)3 | 107.6 (15) |
| | | H(C)2—C—H(C)3 | 108.8 (15) |

symmetry elements of the space group $P2_1/c$, the four molecules in the cell are outer with an equimolar proportion of isomers (forms 3 and 6 in Fig. 3).

Moreover, in the gaseous state the values found in the literature for $\theta$ vary from 83.3 to 92°, which agrees well with our determination ($\theta$ = 82°) in the solid state.

Strong intermolecular interactions may explain why the outer conformation found in the solid state differs from the inner one frequently assumed in the liquid and gaseous states. Energy calculations or simulations may be of interest to proceed one step further.

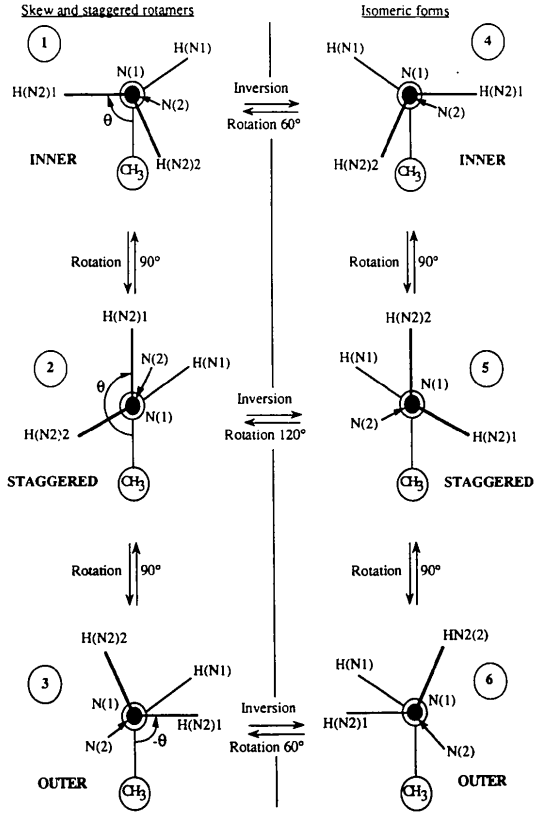


Fig. 3. Different rotamers and isomers of methylhydrazine.

3.2.2. *Packing*. Using an integration method (Foulon, 1987) which takes into account the van der Waals radii ($R_H$ = 1.20, $R_N$ = 1.40 and $R_C$ = 1.80 Å), the molecular volume was estimated to be 48.9 Å$^3$. This value leads to a high compactness factor (0.68).

A perspective view of the structure, nearly parallel to the $b$ axis, is drawn in Fig. 5. The structure may be described as two different planes, $P1$ and $P2$ spaced by 1/2 **a** and parallel to ∠(**b**,**c**). The N(1)—C bonds are nearly parallel to **a**.

Two 'planes' of molecules are weakly linked by van der Waals contacts involving either two methyl or two amine groups in staggered geometry. Each plane contains an equimolar proportion of isomers. One molecule is linked to four neighbours by weak hydrogen bonds. As in the stable phase of hydrazine (Foulon, 1994), one H atom of an amine group is not

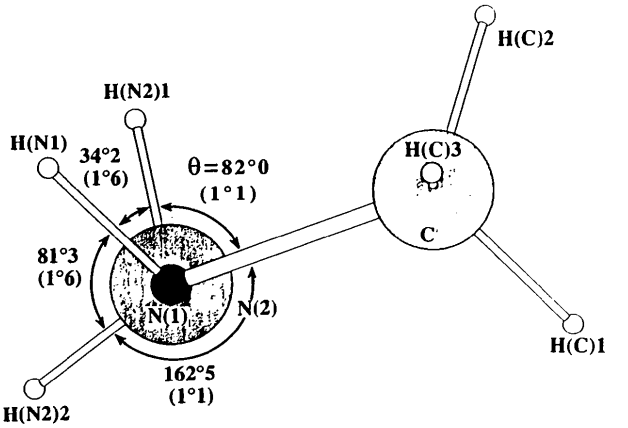


Fig. 4. Newman molecular projection along the N(1)—N(2) bond in the solid state.

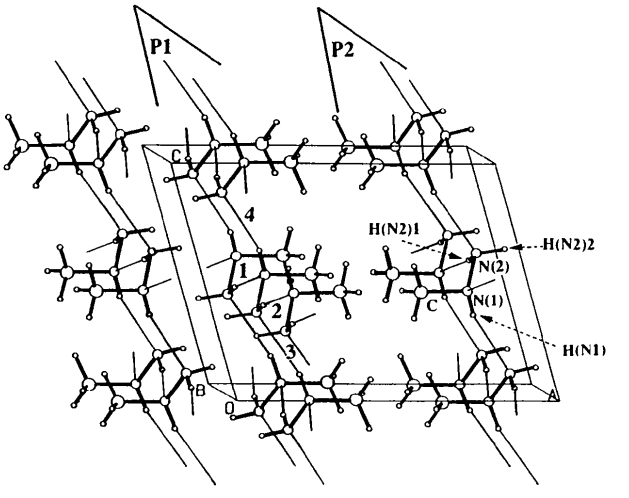


Fig. 5. Perspective view of the structure.

linked in these hydrogen bonds. The hydrogen bonds (denoted by 1, 2, 3 and 4 in Fig. 5) are almost parallel to the **b** (1 and 2) and **c** axes (3 and 4), respectively

bonds 1 and 2 = 2.36 Å

– intermolecular angle 169.8°;

bonds 3 and 4 = 2.29 Å

– intermolecular angle 160.7°.

N(1) and N(2) of one molecule are at once acceptor and donor.

Molecular associations in the liquid phase (Cohen-Adad, El Allali & Getzen, 1987) may be perhaps correlated to these molecular interactions in the solid phase. Furthermore, the geometry of hydrogen bonds in the solid state may furnish a starting model to interpret X-ray scattering experiments in the liquid phase.

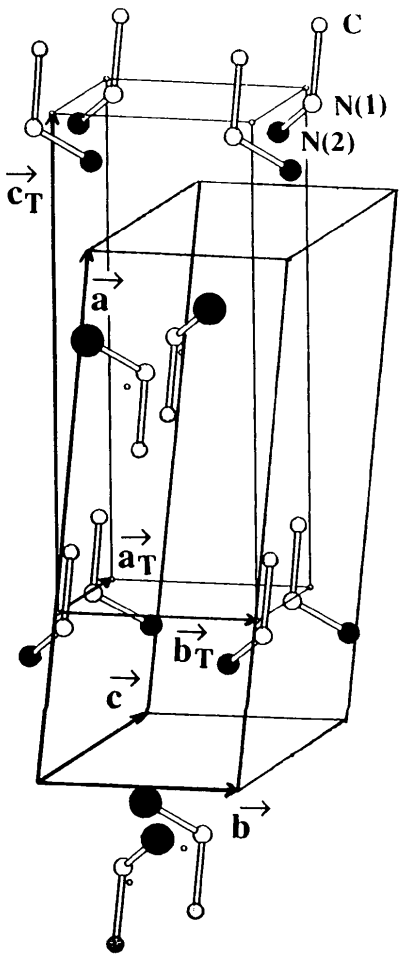


Fig. 6. Simplified view of molecular orientations in the pseudo-quadratic lattice.

3.3. *Simulation of a transition phase at higher temperature*

DSC measurements showed that the metastable phase transforms rapidly into a stable phase during cooling. The rapidity prevents any time-dependent experiments such as a structural analysis on a single crystal of the metastable phase. The first hypothesis to describe this phase is to assume that the two lattices are linked by simple relations. In this way one can estimate the molecular displacements and then simulate the phase transition.

A pseudo-quadratic body-centred lattice ($Z = 2$) may be described considering the space group elements of the stable phase and the particular fractional coordinates of the molecular centre of mass ($x_G = 0.21188$; $y_G = 0.61206$; $x_G = -0.00771$).

After a slight molecular displacement (0.45 Å) to $x_G = 0.25$, $y_G = 0.75$ and $z_G = 0.00$, this pseudo-lattice ($\mathbf{a}_T$, $\mathbf{b}_T$, $\mathbf{c}_T$) and the monoclinic lattice (**a**, **b**, **c**) are related by

$$\mathbf{a}_T = \mathbf{c}/2;\ \mathbf{b}_T = \mathbf{b};\ \mathbf{c}_T = \mathbf{a} + \mathbf{c}/2$$

$$\mathbf{a}_T = 3.835,\ \mathbf{b}_T = 3.925,\ \mathbf{c}_T = 9.625\ \text{Å}$$

$$\alpha_T = \gamma_T = 90,\ \beta_T = 84.9 \cong 90°.$$

In each site of this pseudo-quadratic lattice, the molecule can take two different orientations with the N(1)—C bonds parallel and N(1)—N(2) bonds approximately perpendicular (83°). The molecules at sites (0,0,0) and $(\frac{1}{2},\frac{1}{2},\frac{1}{2})$ are related by inversion, which forbids this lattice to be really body-centred.

From the point of view of molecular orientations, this hypothetical structure appears to be disordered. Fig. 6 shows a view of this quadratic structure where only the heavy atoms and the molecular centre of mass (denoted ° on Fig. 6) are drawn.

According to the globular shape of the molecule, dynamical reorientations can describe this disorder.

## References

ASTON, J. G., FINK, H. L., JANZ, G. J. & RUSSELL, K. E. (1951). *J. Am. Chem. Soc.* **73**, 1939–1943.

COHEN-ADAD, M. T., EL ALLALI, I. & GETZEN, F. W. (1987). *J. Sol. Chem.* **16**(8), 659–678.

COLLIN, R. L. & LIPSCOMB, W. N. (1951). *Acta Cryst.* **4**, 10–14.

FERRIOL, M., GUIDICE, M., COHEN-ADAD, M. T., FOULON, M., GUINET, Y., MULLER, M., LEBRUN, N., BUREAU, J. C. & EL WIDADI, T. (1993). *Fluid Phase Equilib.* **86**, 187–200.

FERRIOL, M., LAACHACH, A., COHEN-ADAD, M. T., GETZEN, F. W., JORAT, L., NOYEL, G., HUCK, J. & BUREAU, J. C. (1992). *Fluid Phase Equilib.* **71**, 287–299.

FISCHER, R. X. & TILLMANNS, E. (1988). *Acta Cryst.* C**44**, 775–776.

FOULON, M. (1987). Thèse d'Etat d'Université, no. 747. Université Lille I.

FOULON, M. (1994). Private communication.

FOULON, M., GUINET, Y., MULLER, M., LEBRUN, N. & FONTAINE, H. (1991). *Proceedings of the Second Meeting on Disorder in Molecular Solids*, 24–27 June 1991. Garchy, France.

FOULON, M., MULLER, M., GUINET, Y., LAHLAOUTI, H., OONK, H. A. J. & MILTENBURG, J. C. VAN (1990). *Proceedings of the Conference on Computer Calculations of Phase Diagrams XIX*, 18–22 June 1990. Noordwijkerout, Pays-Bas.

FOULON, M., MULLER, M., DAMIEN, J. C. & GUINET, Y. (1990). *Proceedings of the XVth Congress and General Assembly: International Crystallography*, 19–28 July 1990. Bordeau France.

GERMAIN, G., MAIN, P. & WOOLFSON, M. M. (1971). *Acta Cryst.* A**27**, 368–376.

GUIDICE, M. (1989). Thèse d'Université, Université Lyon I.

JANZ, G. J. & RUSSELL, E. (1949). *J. Chem. Phys.* **17**, 1352–1353.

LAACHACH, A. (1989). Thèse de Doctorat D'Etat ès Sciences, No. 89–21. Université Claude Bernard, Lyon I.

LAACHACH, A., FERRIOL, M., COHEN-ADAD, M. T., HUCK, J., JORAT, L., NOYEL, G., GETZEN, F. W. & BUREAU, J. C. (1992). *Fluid Phase Equilib.* **71**, 301–312.

LATTIMER, P. & HARMONY, M. D. (1970). *J. Chem. Phys.* **53**(12), 4575–4583.

LATTIMER, P. & HARMONY, M. D. (1972). *J. Am. Chem. Soc.* **94**(2) 351–356.

MURASE, N., YAMAMOUCHI, K., EGAWA, T. & KUCHITSU, K. (1991). *J. Mol. Struct.* **242**, 409–419.

MURASE, N., YAMAMOUCHI, K., SUGIE, M., TAKEO, H., MATSUMURA, C., HAMADA, Y., TSUBOI, M. & KUCHITSU, K. (1988). *J. Mol. Struct.* **194**, 301–316.

SHELDRICK, G. M. (1976). *SHELX76. Program for Crystal Structure Determination*. Univ. of Cambridge, England.

STEWART, R. F., DAVIDSON, E. R. & SIMPSON, W. T. (1965). *J. Chem. Phys.* **42**(9), 3175–3187.

ULICH, H., PEISKER, H. & AUDRIETH, L. F. (1935). *Ber. Dtsch. Chem. Ges. B*, **68**, 1677–1682.

WROBEL, J. R. & GRELECKI, C. (1967). *J. Spacecraft*, **4**, 347–353.

YAMAMOUCHI, K., KATO, S., MOROKUMA, K., SUGIE, M., TAKEO, H., MATSUMURA, C. & KUCHITSU, K. (1987). *J. Phys. Chem.* **91**, 828–833.

# Book Reviews

*Works intended for notice in this column should be sent direct to the Book-Review Editor (R. F. Bryan, Department of Chemistry, University of Virginia, McCormick Road, Charlottesville, Virginia* 22901, *USA). As far as practicable, books will be reviewed in a country different from that of publication.*

*Acta Cryst.* (1994). B**50**, 479–480

**Reviews in computational chemistry. Vol. 3.** Edited by K. B. LIPKOWITZ and D. B. BOYD. Pp. xvi + 271. Weinheim: VCH Verlagsgesellschaft, 1992. Price $75.00. ISBN 1-56081-619-8.

This book is the third in a series intended to provide a guide to the rapidly developing field of computer-aided research in chemistry. The book contains four chapters written by experts in the field. It covers optimization methods, the prediction of oligopeptide structures, molecular modelling using NMR data and methods for the evaluation of chemical toxicity. A fifth chapter provides a compendium of molecular modelling software. The book is intended to provide a tutorial to novices, and a review for experts, of the theoretical background, the implementation methods and the advantages and disadvantages of popular computational chemistry approaches.

A knowledge of optimization methods and their limitations is necessary for any structural chemist who plans to use computational methods. These topics are covered in chapter 1 (71 pp., 142 references) by Tamar Schlick of New York University. He covers essential aspects of the subject, beginning with mathematical preliminaries and moving to search techniques and local and global methods of large-scale optimization, with an explanation of local descent methods and several varieties of minimization methods. This exposition is followed by examples of the performance of various minimization routines. The chapter is comprehensive and, in principle, should provide the education needed by users. However, the explanations are couched in mathematical symbolism rather than in words so that, while the chapter will be useful to the expert seeking a review of methods and implementation strategies, the novice who wishes to understand the basic function of these methods may not be particularly well served.

Chapter 2 (69 pp., 251 references), by Harold Scheraga of Cornell University, is optimistically entitled 'Predicting three-dimensional structures of oligopeptides'. The chapter presents a detailed overview of the computational approaches adopted by the author and his co-workers, with only a cursory and generally critical discussion of alternative approaches to computing such structures or to solving the multiple-minima problem. There are summaries of the theoretical basis for the potential energy calculations used to predict structure, the build-up method of generating an oligopeptide chain and comparisons of computations with experimental observations. The presentation of the theory behind different potential functions and the methods available for treating hydration and entropy effects is clear, precise and useful.

Chapter 3 (49 pp., 121 references), by A. E. Torda and W. F. van Gunsteren of the ETH Zentrum, Zurich, presents the computational aspects of modelling a molecular structure based on nuclear magnetic resonance (NMR) data. The focus is on the determination of protein structure. The authors present the mathematical models for the experimental data and follow with an exposition of methods for refinement and minimization of the molecular model. They successfully bridge the gap between the novice reader and the expert, providing tuition for the former and a rich presentation of the state of the art of minimization and model development for the latter. The chapter provides a clear assessment of the errors and biases of the method and is instructive to the beginning user of molecular dynamics approaches. The presentation is clear and educational, and meets the objectives of the series.

Chapter 4 (49 pp., 227 references), by D. V. F. Lewis of the University of Surrey, presents computational approaches developed for the prediction of the toxicity of newly devel-